Pergamon

Applied Geochemistry, Vol. 9, pp. 353–369, 1994

0883–2927/94 $7.00 + 0.00

0883–2927(94)E0013–U

Geochemical interactions between constituents in acidic groundwater and alluvium in an aquifer near Globe, Arizona

KENNETH G. STOLLENWERK
U.S. Geological Survey, M.S. 413, Box 25046, Federal Center, Denver, CO 80225, U.S.A.

(*Received* 5 *July* 1993; *accepted in revised form* 12 *February* 1994)

Abstract—Acidic water from a copper-mining area has contaminated an alluvial aquifer and stream near Globe, Arizona. The most contaminated groundwater has a pH of 3.3, and contains about 100 mmol/l SO_4, 50 mmol/l Fe, 11 mmol/l Al and 3 mmol/l Cu. Reactions between alluvium and acidic groundwater were first evaluated in laboratory column experiments. A geochemical model was developed and used in the equilibrium speciation program, MINTEQA2, to simulate breakthrough curves for different constituents from the column. The geochemical model was then used to simulate the measured changes in concentration of aqueous constituents along a flow path in the aquifer.

The pH was predominantly controlled by reaction with carbonate minerals. Where carbonates had been dissolved, adsorption of H^+ by iron oxides was used to simulate pH. Acidic groundwater contained little or no dissolved oxygen, and most aqueous Fe was present as Fe(II). In the anoxic core of the plume, Fe(II) was oxidized by MnO_2 to Fe(III), which then precipitated as $Fe(OH)_3$. Attenuation of aqueous Cu, Co, Mn, Ni and Zn was a function of pH and could be quantitatively modeled with the diffuse-layer, surface complexation model in MINTEQA2. Aluminum precipitated as amorphous $Al(OH)_3$ at pH >4.7 and as $AlOHSO_4$ at pH <4.7. Aqueous Ca and SO_4 were close to equilibrium with gypsum.

After the alluvium in the column had reached equilibrium with acidic groundwater, uncontaminated groundwater was eluted through the column to evaluate the effect of reactants on groundwater remediation. The concentration of Fe, Mn, Cu, Co, Ni and Zn rapidly decreased to the detection limits within a few pore volumes. All of the gypsum that had precipitated initially redissolved, resulting in elevated Ca and SO_4 concentrations for about 5 pore volumes. Aluminum and pH exhibited the most potential for continued adverse effects on groundwater quality. As H^+ desorbed from $Fe(OH)_3$, pH remained below 4.5 for more than 20 pore volumes, resulting in dissolution of $AlOHSO_4$ and elevated aqueous Al.

INTRODUCTION

CONTAMINATION of groundwater by wastes generated from the mining and extraction of metals from ore deposits is a problem in many parts of the world. Processes that affect the mobility of these wastes are commonly evaluated with geochemical computer programs; however, the usefulness of these programs is typically limited by a lack of adequate field data. Gaps in field measurements can be supplemented with data from laboratory column experiments designed to simulate transport and chemical reactions in the aquifer.

The objective of this study was to characterize the reactions that control mobility of constituents in the plume of acidic water that has contaminated the alluvial aquifer and stream in Miami Wash and Pinal Creek, Arizona. Laboratory experiments were used in conjunction with ground- and surface-water analyses to develop a geochemical model of the aquifer that described the measured changes in chemical composition.

DESCRIPTION OF STUDY AREA

Geology and hydrology

The study area is in the Pinal Creek drainage basin and includes most of the Globe-Miami mining district near the town of Globe, Arizona (Fig. 1). Topography of the region is characterized by block-faulted mountains and valleys that range in elevation from 670 to 2400 m above sea level. Ore minerals are primarily hydrothermal in origin and are disseminated in granite porphyry. Copper has been the predominant metal mined from the area, although lesser amounts of several other metals also were produced. Large-scale Cu production began in the early 1900s and continues to the present.

The primary aquifer in the basin consists of two units. An unconsolidated alluvium in a band 300–800 m wide, 20 km long and as much as 50 m thick forms the upper, central part of the aquifer in a valley along Miami Wash and Pinal Creek (Fig. 1) (EYCHANER, 1989). The alluvium consists predominantly of more

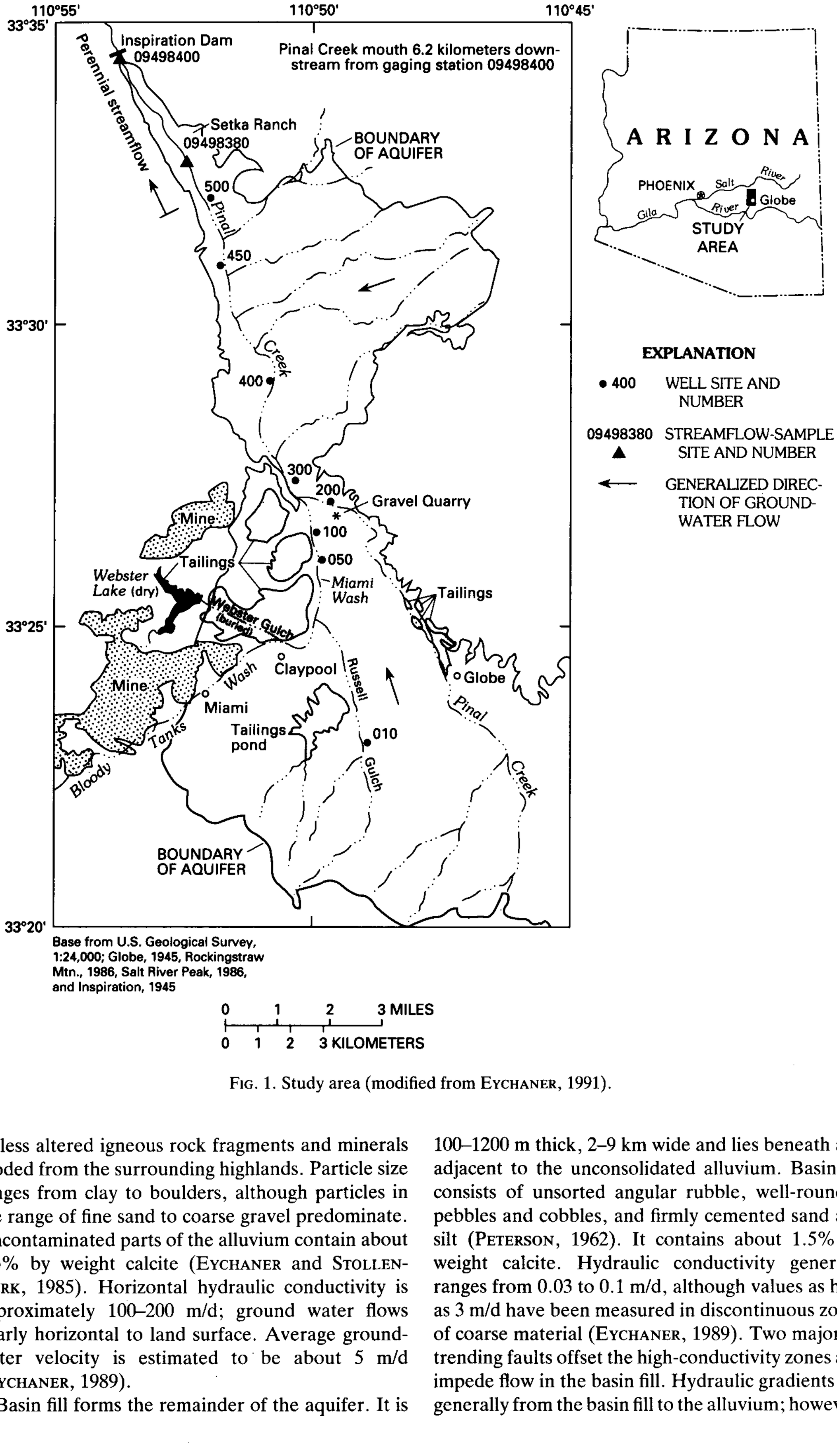

FIG. 1. Study area (modified from EYCHANER, 1991).

or less altered igneous rock fragments and minerals eroded from the surrounding highlands. Particle size ranges from clay to boulders, although particles in the range of fine sand to coarse gravel predominate. Uncontaminated parts of the alluvium contain about 0.3% by weight calcite (EYCHANER and STOLLENWERK, 1985). Horizontal hydraulic conductivity is approximately 100–200 m/d; ground water flows nearly horizontal to land surface. Average groundwater velocity is estimated to be about 5 m/d (EYCHANER, 1989).

Basin fill forms the remainder of the aquifer. It is 100–1200 m thick, 2–9 km wide and lies beneath and adjacent to the unconsolidated alluvium. Basin fill consists of unsorted angular rubble, well-rounded pebbles and cobbles, and firmly cemented sand and silt (PETERSON, 1962). It contains about 1.5% by weight calcite. Hydraulic conductivity generally ranges from 0.03 to 0.1 m/d, although values as high as 3 m/d have been measured in discontinuous zones of coarse material (EYCHANER, 1989). Two major E-trending faults offset the high-conductivity zones and impede flow in the basin fill. Hydraulic gradients are generally from the basin fill to the alluvium; however,

the basin fill is an important source of water in the region and excessive pumping can locally reverse the hydraulic gradient. Most of the contamination has occurred in the unconsolidated alluvium and uppermost part of the basin fill.

Mean annual precipitation in the region ranges from 340 to 780 mm/a (SELLERS *et al.*, 1985); precipitation occurs as brief summer thunderstorms or light, steady winter rains that may continue for several days. Snow accumulates above 2000 m. Most recharge to the aquifer occurs during winter and spring. Surface-water flow in most of the basin is intermittent throughout the year although there is substantial groundwater flow. Perennial flow in Pinal Creek begins approximately 16 km downstream from Globe where low permeability rocks constrict the aquifer and force groundwater flow to the surface. Measured baseflow at a streamflow-gauging station at the north end of the study area is about 0.3 m^3/s (EYCHANER *et al.*, 1989). About 6 km downstream from the gauging station, Pinal Creek discharges to the Salt River which drains into a reservoir that provides water for irrigation of cropland in Maricopa County and is a supplemental public water supply for Phoenix, Arizona.

Description of plume

The most likely sources of contamination are the acidic lake in Webster Gulch (Fig. 1) and perhaps smaller acidic ponds in the area (ENVIROLOGIC SYSTEMS, INC., 1983). From at least 1940 through to 1986, acidic mining and milling-process solutions were discarded in the unlined lake formed by blockage of the natural drainage of Webster Gulch with mill-tailings. In 1986, the volume of water in Webster Lake was about 5.5×10^6 m^3, the concentration of total dissolved solids was 35,000 mg/l, and pH was 2.7 (EYCHANER, 1988). The U.S. Environmental Protection Agency (USEPA, 1987) ordered Webster Lake drained, and by May 1988 the lake water had been spread on inactive tailings to evaporate. Other potential sources of contamination in the area include old, inactive mining facilities and hundreds of abandoned mines; however, contamination from these sources is considered to be minor and only local in effect (ENVIROLOGIC SYSTEMS, INC., 1983).

Seepage of acidic water from Webster Lake through the former channel of Webster Gulch apparently enters the alluvial aquifer near the confluence of Bloody Tanks Wash and Russell Gulch (Fig. 1). As the plume travels northward, aqueous constituents are attenuated by reaction with the alluvium. Aqueous concentrations also decrease via dilution with uncontaminated water. Primary inflows of uncontaminated groundwater are from Russell Gulch and Pinal Creek. The plume is also diluted by groundwater flowing upward from the basin fill and by direct infiltration of surface-water after precipitation. In all cases, mixing is not necessarily instantaneous, and uncontaminated water can flow parallel to the plume for hundreds of meters before complete mixing occurs.

The plume of contaminated groundwater is characterized by a series of chemical fronts that are defined by the geochemistry of individual constituents. The location of the contaminant plume in 1988, as defined by pH, is represented in Fig. 2, a longitudinal section of the aquifer from Webster Lake to Inspiration Dam. Most acidic contamination is within the unconsolidated alluvium; however, the water chemistry of the upper part of the basin fill also has been affected. The shape of the contaminant plume is actually three-dimensional, with the reaction front extending not only in the longitudinal direction with flow, but also in the vertical and transverse directions to flow (WALTER and NORRIS, 1991).

On the basis of groundwater composition, the aquifer can be divided into three generalized zones; acidic, neutralized and uncontaminated. Uncontaminated groundwater contains dissolved oxygen, has nearly neutral pH and is low in dissolved solids (Table 1). Groundwater in the core of the most contaminated portion of the aquifer, is depleted in oxygen and is characterized by low pH and large concentrations of dissolved metals and sulfate (Table 1). The large concentration of SO_4 in acidic groundwater has a significant effect on the speciation of aqueous cations. Approximately 50% of the Ca, Mg, Fe, Mn, Cu, Co, Ni and Zn in contaminated groundwater is transported as SO_4-ion pair complexes, and more than 80% of the Al is complexed with SO_4 (Table 2). The front of acidic water, pH < 5, has advanced through the alluvium at a rate of 0.2–0.3 km/a during the past several decades (EYCHANER, 1991). Neutralized groundwater, defined as having pH values >5, forms a three-dimensional shell of variable extent around the acidic core. Concentrations of most dissolved metals are low; however, Ca, Mg, Mn, Cl and SO_4 concentrations are substantially greater than uncontaminated ground water (Table 1). Neutralized groundwater has reached the gauging station at Inspiration Dam where dissolved solids have been increasing since at least 1942 (ENVIROLOGIC SYSTEMS, INC., 1983; EYCHANER, 1988).

METHODOLOGY

Sampling and analytical techniques

The U.S. Geological Survey began to study contaminant transport in Miami Wash and Pinal Creek in the spring of 1984. Eight groups of observation wells were installed near the stream channels to monitor water level and chemistry (Fig. 1). Each group contained as many as five wells completed at depths from 5 to 69 m. The wells were cased with polyvinyl chloride pipe. The screened interval in most wells is 0.9 m long. Thirteen surface-water sites also were monitored at least twice. EYCHANER *et al.* (1989) and BROWN (1990) describe the details of well construction and sample

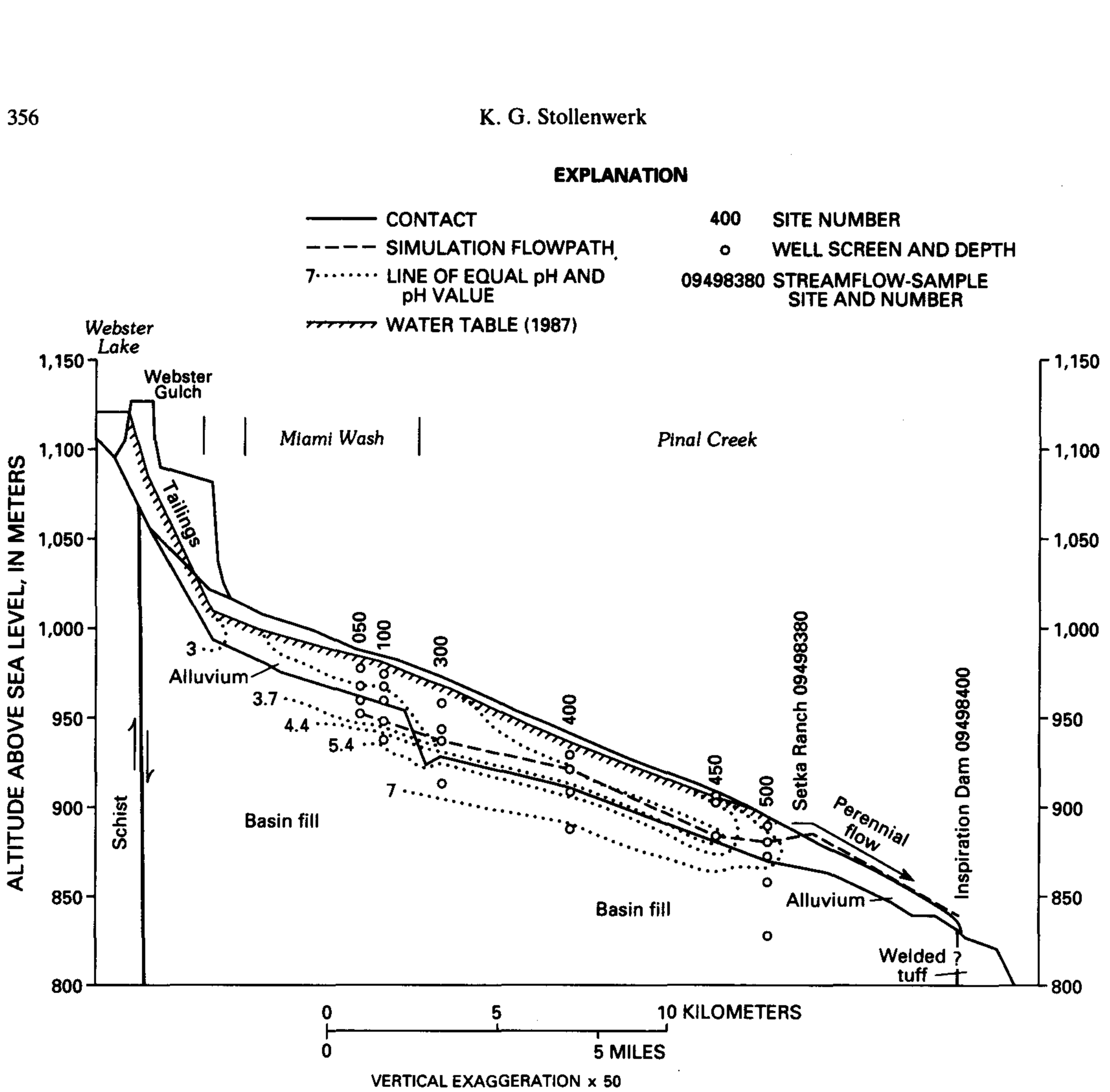

FIG. 2. Distribution of pH in aquifer (modified from EYCHANER, 1991).

Table 1. Range in concentration (mmol/l) of constituents in water from the alluvial aquifer. pH in standard units and Eh in millivolts (mV)

Constituent	Uncontaminated groundwater*	Contaminated groundwater	Neutralized surface water from Inspiration Dam
pH	7.19	3.30	7.95
Eh	—	430	—
Temperature (°C)	17	18	25
Dissolved oxygen (O_2)	0.22	<0.006	0.24
Ca	1.2	11.6	14.0
Mg	0.37	15.8	5.6
Na	0.96	9.4	3.4
K	0.03	0.2	0.1
Fe	<0.0007	52.4†	<0.0007
Mn	<0.0006	1.34	0.47
Al	<0.004	10.5	<0.004
Cu	<0.0003	2.4	<0.0003
Co	<0.001	0.20	<0.001
Ni	<0.002	0.06	<0.002
Zn	<0.0005	0.33	<0.0005
SO_4^{2-}	0.70	100	20
Cl^-	0.48	9.5	2.8
HCO_3^-	2.3	0	3.3
Ionic strength	4.2	232	57
Ionic balance (%)	−1.0	−0.6	1.1

*Uncontaminated groundwater from well 202; contaminated ground water from well 051; neutralized surface water from gauging station 09498400 at Inspiration Dam.

†Fe(II) is 97% or more of total Fe.

Table 2. Speciation of selected constituents in water samples from Table 1*

Species	Uncontaminated groundwater (%)	Contaminated groundwater (%)	Neutralized surface water (%)
Ca^{2+}	91	52	65
$CaSO_4^0$	5	48	33
Mg^{2+}	90	54	67
$MgSO_4^0$	5	46	30
Na^+	100	94	97
$NaSO_4^-$	0	6	3
Fe^{2+}	—	59	—
$FeSO_4^0$	—	41	—
Mn^{2+}	—	57	68
$MnSO_4^0$	—	42	29
Al^{3+}	—	16	—
$AlSO_4^+$	—	40	—
$Al(SO_4)_2^-$	—	44	—
Cu^{2+}	—	53	—
$CuSO_4^0$	—	47	—
Co^{2+}	—	50	—
$CoSO_4^0$	—	50	—
Ni^{2+}	—	57	—
$NiSO_4^0$	—	43	—
Zn^{2+}	—	41	—
$ZnSO_4^0$	—	41	—
$Zn(SO_4)_2^{2-}$	—	18	—

*Speciation calculated by MINTEQA2 (Allison *et al.*, 1991).

collection and list all ground- and surface-water analyses from 1984 through 1989.

Most groundwater samples were collected using a submersible pump. Water samples were collected only after at least three casing volumes of water had been removed and the pH, specific conductance, temperature and dissolved-oxygen concentration had stabilized. Both ground- and surface-water samples were filtered through a 0.45-μm membrane filter and stored in polyethylene bottles. Preliminary experiments on sampling methodology found no significant concentration of colloids >0.03 μm in size (Eychaner and Stollenwerk, 1985). Samples submitted for cation analysis were acidified with ultra-pure HNO_3 to a pH of approximately 1.5. Samples for anion analysis were unacidified. All samples were packed in ice for shipment and stored in a refrigerator until analyzed in the author's laboratory. Random replicates also were analyzed by the U.S. Geological Survey National Water Quality Laboratory to ensure quality control. An ionic balance for each sample was computed as:

$$\frac{\text{sum cations (meq/l)} - \text{sum anions (meq/l)}}{\text{sum cations (meq/l)} + \text{sum anions (meq/l)}} \times 100\%.$$

Any sample that did not achieve an ionic balance within ±10% was reanalyzed. The maximum analytical error for all analyses reported in this paper is ±10% at the 95% confidence interval.

Cations were determined with a Jarrell-Ash Atom Comp 975 inductively coupled atomic-emission spectrophotometer. (Use of brand names in this paper is for identification purposes only and does not constitute endorsement by the U.S. Geological Survey.) Chloride was determined by the ferric thiocyanate method and sulfate by the turbidimetric method (USGS, 1989). Ferrous and ferric iron were measured using the bipyridine colorimetric procedure (USGS, 1979). Separation between Fe(II) and Fe(III) could not be quantified if the concentration of either was <3% of total Fe. Dissolved oxygen was measured by probe, pH by glass electrode, and Eh with a polished platinum electrode and a silver–silver chloride reference electrode that was calibrated with Zobell's solution between measurements. The carbonate content of the alluvium was determined by the Chittick method (Dreimanis, 1962). Oxides of Mn and Fe were sequentially extracted from samples of alluvium. Manganese oxides were dissolved using 0.1 N hydroxylamine hydrochloride ($NH_2OH \cdot HCl$) in 0.01 N HNO_3 and shaking for 30 min (Chao, 1972). Amorphous iron oxides were dissolved in a solution of 0.25 N $NH_2OH \cdot HCl$ and 0.25 N HCl at 50°C for 30 min (Chao and Zhou, 1983). Crystalline iron oxides were dissolved in 4.0 N HCl at 90°C for 30 min (Ficklin *et al.*, 1991).

Column experiments

Controlled, laboratory column experiments were used to identify reactions between groundwater and alluvium. Plexiglass columns, 80 cm long by 5 cm inside diameter, were packed with the <2-mm-size fraction of alluvium. The <2-mm-size fraction comprised between 70 and 80% of the total weight of the alluvium samples. Porosities ranged from 31 to 32%. Four experiments were run, each with a different sample of alluvium or basin fill. Breakthrough of individual constituents varied between columns and was primarily a function of the initial carbonate content. Results from only one column are presented in this paper. The material used in this column was collected from a gravel quarry in the unconsolidated alluvium just upstream from site 200 (Fig. 1). This sampling site was necessary because zones of relatively large cobbles in the aquifer prevented collection of representative core samples for use in the laboratory experiments. Several samples were collected from the exposed sections of alluvium in the quarry and composited. Petrographic examination showed no observable difference in mineralogy between the composite sample and cuttings obtained from uncontaminated alluvium during drilling of the observation wells. Both alluvial samples contained about 35% quartz, 10% feldspar, 25% metamorphic rock fragments, 10% granite, 10% volcanics, 5% biotite and muscovite, and 2% magnetite. In addition, preliminary

batch experiments, conducted to test the reactivity of the composite sample and cuttings towards acidic groundwater, measured no difference. Therefore, the composite sample from the gravel quarry was assumed to be representative of the physical and chemical state of the unconsolidated alluvium in the aquifer prior to contamination.

An initial baseline was established by eluting uncontaminated groundwater collected from well 202 (Table 1) through the alluvium until there was no change in the concentration of dissolved constituents. Column influent was then switched to groundwater collected from a well screened in the core of the acidic plume (well 051, Table 1). This water had been filtered into Pyrex bottles and refrigerated until used. Acidic water was pumped through the alluvium until complete breakthrough of all constituents was achieved (effluent concentration = influent concentration). Approximately 9 pore volumes of acidic water were required for complete breakthrough. Influent was then switched back to uncontaminated groundwater to evaluate the restoration of water quality to pre-contamination levels.

A peristaltic pump was used to control flow through the columns in an upward direction at an average velocity of 0.4 m/d. This velocity is less than the 5 m/d estimated for the aquifer (EYCHANER, 1989); however, a slower velocity in the column was required because of the short travel distance. Effluent was filtered through inline 0.4-μm polycarbonate membrane filters as it exited from the columns and was collected in an automatic fraction collector. The entire experimental apparatus was enclosed in a glove box that contained an anoxic nitrogen atmosphere to simulate the reducing conditions in the core of the plume. The pH and concentration of anions in effluent fractions were measured daily. Samples to be analyzed for cations were acidified with ultra-pure HNO_3 and stored in a refrigerator until analyzed.

GEOCHEMICAL MODELING

A geochemical model was developed to simulate the measured concentration of constituents in column effluent. The intent was to find a minimum set of chemical reactions that would explain the observed breakthrough of constituents. Local equilibrium was assumed for all reactions (BAHR and RUBIN, 1987).

Reactions were simulated with the geochemical computer program MINTEQA2 (ALLISON *et al.*, 1991). The MINTEQA2 thermodynamic data bases were updated with current chemical equilibrium constants from NORDSTROM *et al.* (1990). Equilibrium constants for Co were calculated using thermodynamic data from NAUMOV *et al.* (1974). If the necessary parameters were available, activity coefficients were calculated using the modified Debye–Huckel equation, otherwise, the Davies equation was used.

Adsorption

The aqueous concentration of H, Mn, Cu, Co, Ni and Zn were controlled by pH-dependent adsorption on oxide minerals. These reactions were simulated using the diffuse-layer surface complexation model (DZOMBAK and MOREL, 1990) in MINTEQA2. Parameters that are required by the model include the mass of adsorbent, its specific surface area and the concentration of adsorption sites. At least one adsorption reaction and an equilibrium constant must be defined for each constituent. Surface charge and potential are computed by MINTEQA2.

Table 3. Adsorption parameters for the diffuse-layer model for adsorption on $Fe(OH)_3$

$Fe(OH)_3$ properties	
Specific surface area = 600 m^2/g	
Concentration of adsorption sites = 0.2 mols/mol Fe*	
Concentration $Fe(OH)_3$ = 10.4–12.5 g/kg†	
Surface complexation reactions	**Log *K***
(1) $\equiv FeOH^0 + H^+ = \equiv FeOH_2^+$	7.29‡
(2) $\equiv FeOH^0 = \equiv FeO^- + H^+$	−8.93‡
(3) $\equiv FeOH^0 + Cu^{2+} = \equiv FeOCu^+ + H^+$	0.6§
(4) $\equiv FeOH^0 + Co^{2+} = \equiv FeOCo^+ + H^+$	−2.0‖
(5) $\equiv FeOH^0 + Ni^{2+} = \equiv FeONi^+ + H^+$	−2.5§
(6) $\equiv FeOH^0 + Zn^{2+} = \equiv FeOZn^+ + H^+$	−1.99‡
(7) $\equiv FeOH^0 + Mn^{2+} = \equiv FeOMn^+ + H^+$	−2.6‖

$\equiv FeOH^0$ is a surface complexation site.

*For conversion from g/l $Fe(OH)_3$ to mol/l Fe, DZOMBAK and MOREL (1990) assumed a stoichiometry of 89 g/mol Fe.

†Sum of $Fe(OH)_3$ initially present in alluvium plus $Fe(OH)_3$ precipitated from solution.

‡Log *K* computed by DZOMBAK and MOREL (1990), based on literature review.

§Log *K* computed by DZOMBAK and MOREL (1990), based on linear free energy relationships.

‖Log *K* by empirical fit to column data.

The alluvium contained a mixture of potential adsorbents. Iron oxides were expected to dominate adsorption reactions because all of the grains in core samples were visibly coated with reddish Fe oxides, even in uncontaminated alluvium. In addition, large amounts of Fe(II) were oxidized to Fe(III) and precipitated from the acidic plume. Manganese and Al oxides are also present in the alluvium and are potentially important adsorbents; however it was not possible to separate the effect of Mn and Al oxides from Fe oxides. Therefore, all adsorption reactions were assumed to occur on ferrihydrite [$Fe(OH)_3$].

Adsorption parameters for the diffuse-layer model are listed in Table 3. The concentration of $Fe(OH)_3$ was calculated by adding the amount of "amorphous iron oxides", determined by chemical extraction of the alluvium, to the amount of $Fe(OH)_3$ that precipitated from solution as acidic groundwater moved through the column or aquifer. Thus, the concentration of $Fe(OH)_3$ used in the simulations increased proportionally with the amount that precipitated. The surface area of 600 m^2/g and the adsorption site density of 0.2 mol/mol Fe were used for consistency with DZOMBAK and MOREL (1990). The equilibrium constants for H, Cu, Ni and Zn (Table 3) were taken from DZOMBAK and MOREL (1990). They are based on

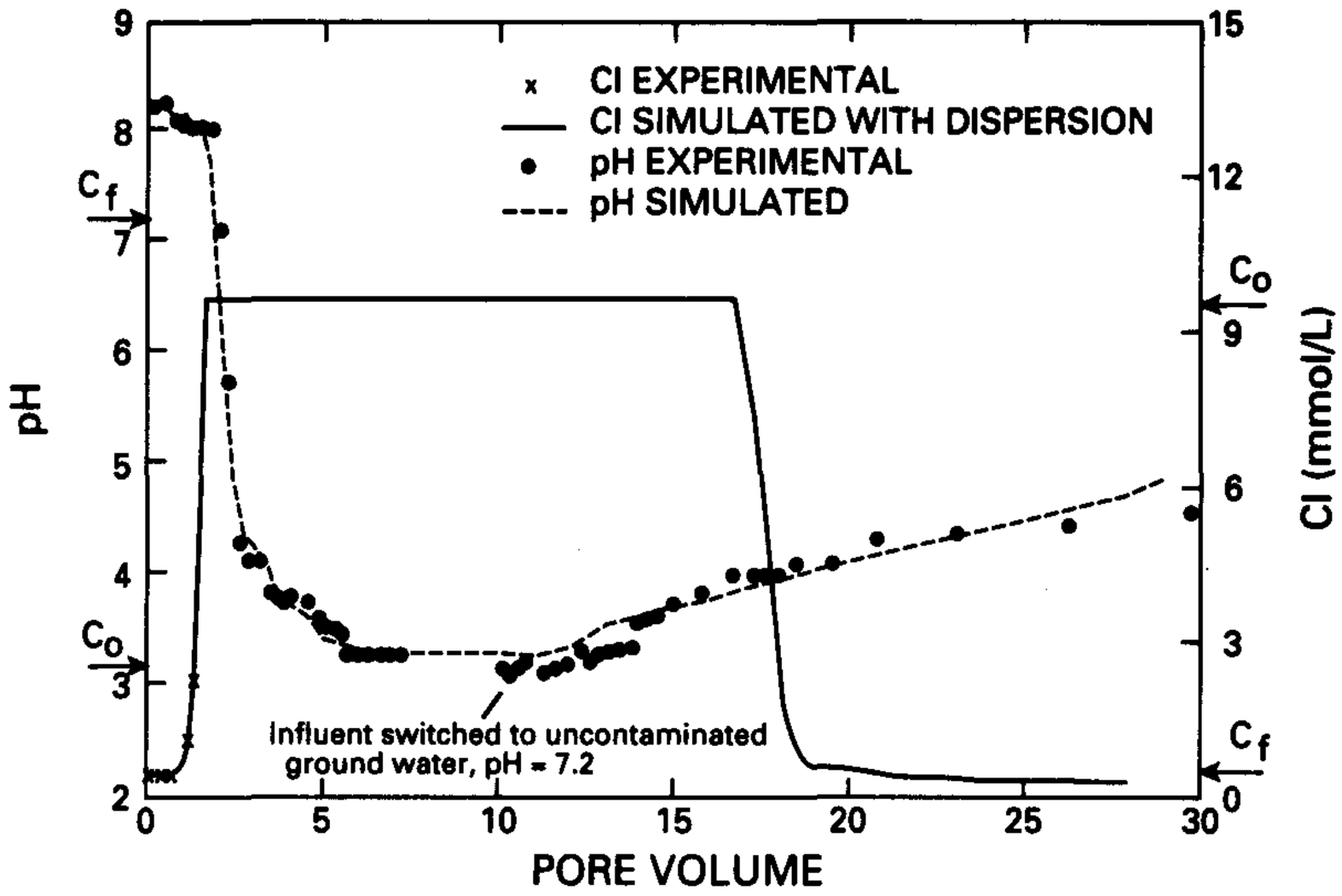

FIG. 3. Experimental and simulated pH and Cl concentration in column effluent. For this and all subsequent figures, C_o = concentration in contaminated water influent, and C_f = concentration in uncontaminated water influent.

an extensive compilation and interpretation of published experimental data for adsorption of ions by $Fe(OH)_3$. The published log K values for Co and Mn were modified to fit the data from the column experiments.

Dispersion and dilution

Dispersion in the column is evident from the shape of the breakthrough curve for non-reactive Cl (Fig. 3). A dispersivity of 0.12 m was calculated for the Cl data. The shape of the ascending limb of the breakthrough curve for constituents other than Cl was dominated by chemical reactions, and dispersion was disregarded in the simulations. There was more dispersion in the rinse-out of constituents from the column. In fact, the shape of the descending limb of the breakthrough curve for some constituents was dominated by dispersion; therefore, all simulations of the rinse-out of constituents from the column were manually corrected to reflect the amount of dispersion determined from the Cl data.

After the column breakthrough curves were simulated by MINTEQA2, the geochemical model was tested on the data set from the aquifer. This required choosing an appropriate flow path. In contrast to the one-dimensional flow system of the column, there is a three-dimensional aspect to the plume and flow system in the aquifer. The flow path chosen (Fig. 2) connects the most contaminated well in each of six observation well nests and two surface water sampling sites on Pinal Creek, Setka Ranch and Inspiration Dam. This flow path offers a continuous progression from the most contaminated well, 051, to the least contaminated surface-water at the gauging station.

The concentration of constituents at most of these observation points was relatively constant for the nine sampling rounds between November 1984 and August 1987, indicating that the observation wells were not located in any zones of rapidly changing chemistry. Therefore, the concentration of each constituent plotted in all of the figures of field data in this paper are an average of the nine sampling rounds. The only exception is well 452, which was not completed until 1988. Data from this site are for only two sampling periods. The associated error bars show the minimum and maximum concentration at each site for the averaged period.

In addition to simulating chemical reactions along this flow path, simulation of the field data also has to account for dilution of constituents in the acidic plume by groundwater from other sources. There is not enough hydrologic data for the Miami Wash–Pinal Creek flow system to determine the location and amount of mixing, so a chemical tracer was used to calculate dilution between wells. The assumption was made that Cl was non-reactive. Therefore, the decrease in Cl concentration along the flow path was assumed to be the result of dilution by uncontaminated ground water. These appear to be reasonable assumptions in that there are no known sources of mineral Cl in the aquifer, and the column data indicated no precipitation or adsorption of Cl.

Dilution of contaminated ground water along the flow path was accomplished by using the mixing option in the geochemical computer program PHREEQE (PARKHURST *et al.*, 1980). The volume of uncontaminated water (well 202, Table 1) added to the model was first calculated from the decrease in Cl concentration between successive sites along the flow path (Fig. 4). The resultant mixed water was then used as the input solution for MINTEQA2. The data

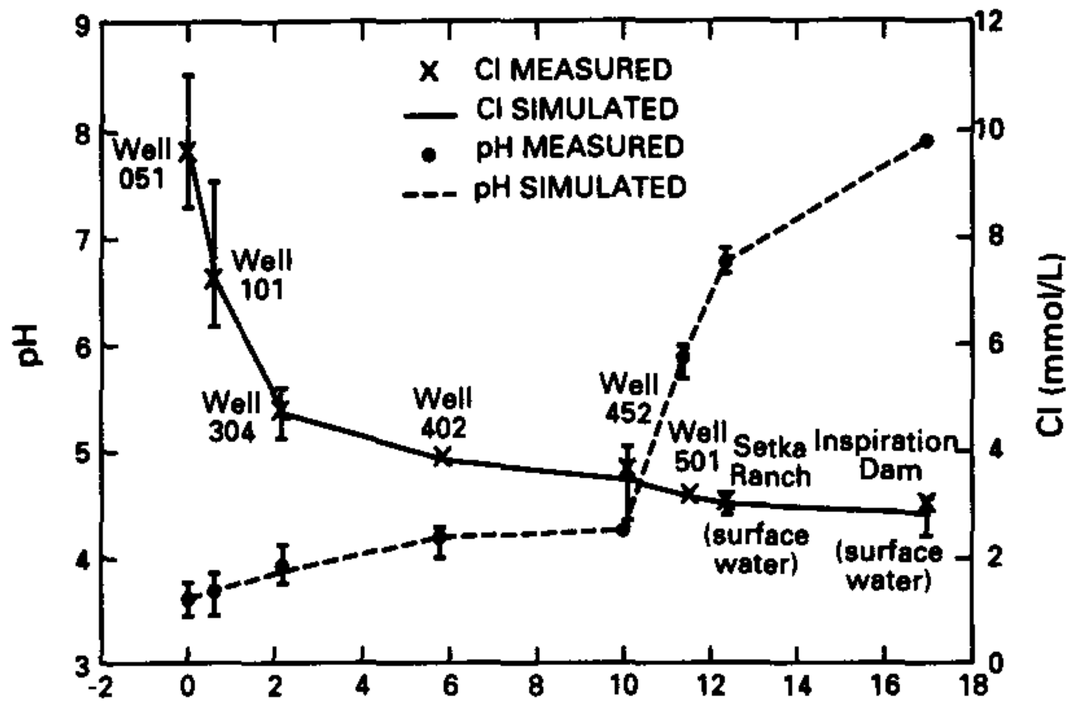

FIG. 4. Measured and simulated pH and Cl concentration at observation points along flow path in aquifer. For Cl, each simulation was fitted to the average measured concentration to determine the amount of dilution between observation points.

in Fig. 4 clearly show that most dilution occurs within the first 2 km, as ground water from Russell Gulch and Pinal Creek mix with the acidic plume.

RESULTS AND DISCUSSION

pH

The concentration of free and complexed H^+ in acidic groundwater (well 051 in Table 1) accounted for only 0.7 mmol/l of the total acidity that can be produced in this sample. Additional H^+ will be produced by hydrolysis of metal ions and exchange of cations for H^+ on oxide surfaces. These reactions, discussed in detail in the following sections, have the potential to produce 114.4 mmol/l of H^+ and will maintain low pH values until these solutes are removed from solution (Table 4).

Experimental and modeled breakthrough curves for the pH of effluent from the column experiment are plotted in Fig. 3. A combination of processes were used to simulate pH. Initially, carbonate minerals in the alluvium buffered pH at approximately 8. The experimentally determined concentration of carbonate in this sample of alluvium was 0.022 mol CO_3/kg. This value is equivalent to 0.22% by weight calcite. A ratio of 90% calcite to 10% dolomite was used, based on the amount of Mg released to solution during the experiment. Both minerals were allowed to react in MINTEQA2 until depleted according to:

$$CaCO_3 + 2H^+ = Ca^{2+} + H_2O + CO_{2(g)} \quad (1)$$

$$MgCa(CO_3)_2 + 4H^+ = Mg^{2+} + Ca^{2+} + 2H_2O + 2CO_{2)g)}. \quad (2)$$

A P_{CO_2} of $10^{-2.9}$ atm was used in the simulations while carbonates were present. This value was computed from the concentration of HCO_3^- measured in the effluent. The rapid pH decrease to 4.4 that was measured in the experimental data coincided with depletion of carbonate minerals in the simulations.

All of the carbonate minerals in the alluvium should have been depleted by the end of the second pore volume; yet, effluent pH continued to decrease for an additional 4 pore volumes. This decrease in pH from 4.4 to the influent value of 3.3 was simulated using a combination of chemical reactions.

The primary mechanism used to control pH between pore volumes 2 and 6 was adsorption of H^+ by oxide minerals (reaction 1, Table 3). Protonation of the oxide surface, $\equiv FeOH_2^+$, becomes significant at lower pH. MINTEQA2 simulations computed that more than 98% of the available $Fe(OH)_3$ complexation sites were saturated with H^+ at pH 3.3.

Aluminum reactions also consumed H^+ at pH <4.7. Amorphous $Al(OH)_3$ precipitated at pH >4.7, and then altered to a basic aluminum sulfate mineral when pH decreased to <4.7. The net reaction is:

$$Al(OH)_3 + 2H^+ + SO_4^{2-} = AlOHSO_4 + 2H_2O. \quad (3)$$

All of the amorphous $Al(OH)_3$ that had initially precipitated, transformed to $AlOHSO_4$ by pore volume 6. The mineralogy of Al is discussed in greater detail in a later section.

Finally, dissolution of $Fe(OH)_3$ at low pH also removed H^+ from solution:

$$Fe(OH)_3 + 3H^+ = Fe^{3+} + 3H_2O. \quad (4)$$

The total amount of $Fe(OH)_3$ that dissolved between pore volumes 2 and 10 was approximately 2% of the total $Fe(OH)_3$ in the column. Most of the dissolution occurred between pore volumes 5 and 10 at pH <3.5.

Another type of reaction that could deplete aqueous H^+ is alteration of silicate minerals such as feldspars:

$$\underset{\text{albite}}{2NaAlSi_3O_8} + 2H^+ + 9H_2O = \underset{\text{kaolinite}}{Al_2Si_2O_5(OH)_4} + 2Na^+ + 4H_4SiO_4. \quad (5)$$

Petrographic examination of thin sections made from alluvium collected during the drilling of observation wells does show that feldspars are partially to completely replaced by clay minerals; however, there was no observable difference in the percent of altered grains between alluvium collected from the core of the plume and alluvium uncontaminated by the acidic groundwater. Thus, much of the silicate mineral alteration probably predates contamination of the aquifer. Any reactions between the acidic groundwater and silicate minerals would proceed at a much slower rate than the other reactions considered above, and would require addition of a kinetic reaction rate term to MINTEQA2. Silicate dissolution was not needed to simulate the pH data from the column experiment; therefore, silicate dissolution was not considered.

The influent solution was changed back to uncon-

Table 4. H^+ production potential for acid-contaminated groundwater from well 051, Table 1

Solute	Process	H^+ produced (mmol/l)
Fe	oxidation and precipitation	52.4
Al	precipitation	31.5
Mn	reduction and adsorption	27.5
Co, Cu, Ni, Zn	adsorption	3.0
Total		114.4

taminated groundwater at pore volume 10. Effluent pH increased very gradually (Fig. 3). Even after 20 pore volumes of pH 7.2 water had eluted through the column, pH was only 4.6. The experimental pH was simulated by allowing dissociation of the $\equiv FeOH_2^+$ surface complex:

$$\equiv FeOH_2^+ = \equiv FeOH + H^+. \quad (6)$$

As a consequence of this reaction, HCO_3^- was removed from uncontaminated groundwater by reaction with H^+. Bicarbonate was not detected in any of the effluent, even though the concentration of HCO_3^- in the influent water was 2.3 mmol/l (Table 1). MINTEQA2 simulations computed that approximately 50% of the surface sites were still populated with H^+ at pore volume 30. Additional simulations, not shown in Fig. 3, predicted that an additional 18 pore volumes of uncontaminated water would need to be eluted through the column to increase pH to 7.2. These results indicate that considerable time may be required to restore the pH of groundwater to pre-contaminant values.

The change in pH of groundwater along the flow path chosen for the aquifer simulations (Fig. 4) was simulated with the same reactions that were used to simulate pH in the column experiment. The acidic core of the plume, characterized by pH <4.5 extended 10 km down-gradient from the starting point of the simulations. Carbonate minerals should have primarily been removed from this reach of aquifer, so pH was simulated by a combination of H^+ adsorption on $Fe(OH)_3$ and neutralization by HCO_3^- in uncontaminated groundwater that mixed with the plume. Reaction with HCO_3^- removed 20% of the total H^+ from solution along the first 10 km; the remainder was adsorbed. Carbonate minerals were assumed to be present in the aquifer only if groundwater pH was greater than 4.5, as was the case between 10 and 12 km. The sharp increase in pH along this reach defined the transition zone between acidic and neutralized groundwater. The actual concentration of carbonate in alluvium between these observation wells could not be determined; therefore, the actual amount of carbonate dissolved between 10 and 12 km was used as a fitting parameter to simulate the measured pH. The ratio of calcite to dolomite (10:1) in the aquifer was assumed to be the same as that used in the column experiment. The pH of the two surface-water sites was near equilibrium with calcite.

Iron

Ferrous iron is the dominant cation in the acidic groundwater; its chemical reactions have a significant effect on the mobility of other solutes. In the column experiment, Fe(II) was completely removed from solution until pore volume 2; then the effluent concentration rapidly increased to the influent concentration of 55 mmol/l (Fig. 5). In fact, the concentration of Fe(II) actually exceeded 55 mmol/l between pore volumes 3 and 4 by as much as 13%. Some Fe(II) may have been adsorbed by the alluvium initially, and was desorbed as the pH decreased. Adsorption of Fe(II) was not considered in the model. Dissolution of $Fe(OH)_3$ was not predicted until pore volume 5.

Experimental and thermodynamic evidence indicate that the most plausible mechanism for attenuation of Fe was oxidation of Fe(II) to Fe(III), followed by precipitation of $Fe(OH)_3$:

$$Fe^{2+} + 3H_2O = Fe(OH)_3 + 3H^+ + e^-. \quad (7)$$

Jarosite $[(H,Na,K)Fe_3(SO_4)_2(OH)_6]$, the only other mineral that was supersaturated with respect to Fe, could not be detected in reacted column alluvium or in cuttings from the aquifer by either X-ray diffraction or electron microprobe, and was not considered in this study. Jarosite supersaturation without precipitation has been reported elsewhere (NORDSTROM *et al.*, 1979). Apparently there is a kinetic inhibition to precipitation of this mineral in some environments.

Reaction (7) requires an electron acceptor. Although there are several potential oxidants that could be considered for this system, most can be excluded. Oxidation of Fe(II) by O_2, NO_3^- and NO_2^- would be thermodynamically favorable, except O_2 was excluded from the column experiment, and the concentrations of NO_3^- and NO_2^- in acidic groundwater were below detection. Sulfate and CO_2 were present in solution; however, oxidation of Fe(II) by these species was computed to be thermodynamically unfavorable. Likewise, independent experiments

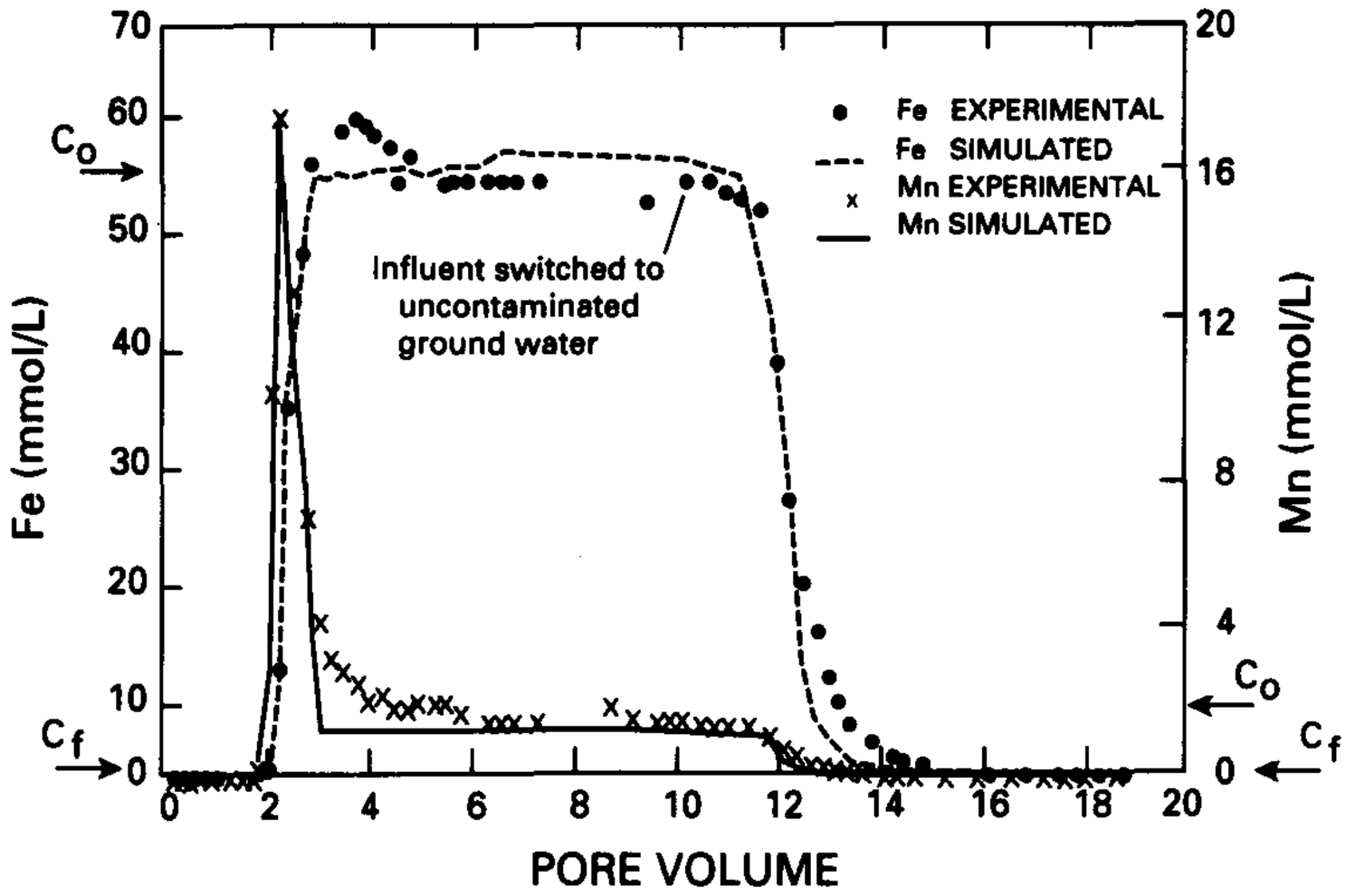

FIG. 5. Experimental and simulated concentration of total dissolved Fe and Mn in effluent from the column experiment. Fe(II) comprises 97% or more of total Fe.

verified that the N_2 atmosphere of the glove box had no effect on the oxidation state of Fe.

The most plausible oxidants in this system are manganese oxide minerals such as birnessite (MnO_2), which are relatively abundant in alluvium that has not been in contact with the acidic plume. Oxidation of Fe(II) by manganese oxides has been described by several investigators. ASGHAR and KANEHIRO (1981) measured an increase in the amount of Mn that could be leached from soil upon addition of Fe(II). Other investigators have found that Fe(II) is readily oxidized by synthetic birnessite [$Mn_7O_{13} \cdot 5H_2O$] (GOLDEN *et al.*, 1986; KRISHNAMURTI and HUANG, 1987). However, no attempt was made to exclude atmospheric O_2 from any of these experiments, which complicates interpretation of reaction rates and stoichiometry. POSTMA (1985) conducted laboratory experiments under a N_2 atmosphere. His results confirmed that synthetic birnessite oxidized Fe(II) in the absence of O_2, yielding a ratio of 1.7 mols of Fe(II) oxidized per mol of Mn(II) produced.

MINTEQA2 simulations indicated that the following overall reaction between the acidic water and alluvium was thermodynamically feasible:

$$2Fe^{2+} + MnO_2 + 4H_2O = 2Fe(OH)_3 + Mn^{2+} + 2H^+. \quad (8)$$

For every 2 mol of Fe(II) oxidized, 1 mol of Mn(II) and 2 mol of H^+ should have been produced. A total of 37 mmol of Fe(II) were removed from solution in the column experiment. This amount is equivalent to 14.2 mmol Fe(II) oxidized/kg alluvium. According to reaction 8, there should have been at least 7.1 mmol/kg of MnO_2 in the alluvium initially to account for the observed Fe(II) oxidation. The actual concentration and oxidation state of Mn oxides in the alluvium were difficult to determine. However, alluvium used in the column experiment had been exposed to oxic conditions for several years, and it is likely that Mn(IV) was the dominant oxidation state (HEM and LIND, 1983).

A semi-quantitative estimate of the Mn oxide content of alluvium was made using sequential chemical extraction. A total of 6.2 ± 0.4 mmol/kg of Mn were measured in the Mn oxide extractable fraction of alluvium. An additional 2.4 ± 0.3 mmol/kg of Mn was associated with amorphous $Fe(OH)_3$. If all of this Mn were available for reaction with Fe(II), then there was a total of 8.6 ± 0.7 mmol Mn oxides/kg alluvium, sufficient to account for the observed oxidation of Fe(II) in the column. Sequential chemical extraction of the reacted alluvium after completion of the column experiment measured a decrease in extractable Mn oxides from 6.2 to 0.23 mmol/kg. Furthermore, a substantial increase in Mn in column effluent was also measured (Fig. 5); although the amount of excess Mn in effluent was less than predicted by reaction (8). Possibly, some Mn coprecipitated with $Fe(OH)_3$. Manganese is discussed in greater detail in the next section.

A separate batch experiment was conducted to quantify reaction (8) under conditions that eliminated the possibility of Mn coprecipitation. The experimental details and results are summarized in Table 5. Briefly, 100 ml of water collected from Webster Lake was mixed with 30 g of alluvium in a N_2 atmosphere. The pH of Webster Lake water was 2.8, acidic enough to prevent precipitation of $Fe(OH)_3$. The Webster Lake sample was collected near the surface at the shore; exposure to atmospheric O_2 resulted in oxidation of much of the Fe(II) to Fe(III). Complete oxidation of Fe(II) in this sample was apparently inhibited by the low pH. As noted by STUMM and MORGAN (1981, p. 467), the rate of conversion of Fe(II) to Fe(III) in aerated solutions is very slow below pH 4.0.

There was no change in the concentration of Fe(III), Fe(II), or Mn in acidic water without the

Table 5. Oxidation of Fe(II) by Mn oxides

Control experiment	Concentration (mmol/l) Initial Fe(II)	Initial Fe(III)	Initial Mn	Final Fe(II)	Final Fe(III)	Final Mn	mol Fe(II) oxidized/ mol Mn dissolved
A*	14	42	1.4	14	42	1.4	0
B†	0	0	0	0	3	0	0
C-1‡	14	42	1.4	0	59	9.2	1.8
C-2‡	14	42	1.4	0	60	9.3	1.8

Procedure: all experiments were conducted in 250-ml Pyrex bottles under a N_2 atmosphere. No attempt was made to exclude light.
*N_2 control: 100 ml Webster Lake water, pH 2.8.
†pH control: 30 g alluvium in 100 ml deionized water, acidified to pH 2.8 with H_2SO_4.
‡Replicates: each beaker contained 30 g alluvium in 100 ml Webster Lake water, pH 2.8.

alluvium, control experiment A. The other control experiment, B, was designed to measure the potential amount of Fe and Mn that could be dissolved from the alluvium by adjusting the pH of a deionized water–alluvium suspension to 2.8 with sulfuric acid. No measurable Mn was dissolved from alluvium at this pH; however, the Fe concentration increased to 3 mmol/l indicating some dissolution of $Fe(OH)_3$. When alluvium was added to the acidic water from Webster Lake, replicates C-1 and C-2, the concentration of Fe(II) decreased from 14 mmol/l to 0 and Fe(III) increased correspondingly. Manganese increased from 1.4 to 9.2 mmol/l. Thus, approximately 1.8 mol of Fe(II) was oxidized per mol of Mn dissolved. This computes to an average oxidation number of 3.8 for Mn in the alluvium.

The initial concentration of MnO_2 used to simulate the experimental data (Fig. 5) was 7.1 mmol/kg. This was the amount required to quantitatively oxidize the 14.2 mmol/kg Fe(II) that was removed from solution and is similar to the concentration of Mn oxides measured by sequential extraction. When influent was changed to uncontaminated water, Fe in the pore water of the alluvium was rapidly rinsed from the column (Fig. 5). Concentrations approached detection limits within 3 pore volumes indicating that essentially all of the Fe that precipitated initially remained in the alluvium.

The concentration of Fe along the flow path chosen to simulate changes in aquifer chemistry is plotted in Fig. 6. Iron concentrations decreased from 53 mmol/l at well 051 to near the limit of detection in groundwater 11 km down-gradient. No dissolved Fe was detected in surface water.

There is evidence that oxidation of Fe(II) by manganese oxides takes place in the aquifer as well. FICKLIN *et al.* (1991) used sequential chemical extraction to identify elements associated with the carbonate, manganese oxide and iron oxide phases of alluvium collected from five split-spoon samples from drill holes in contaminated, neutralized and uncontaminated sections of the aquifer. Their data show that there was very little Mn oxide in alluvium from

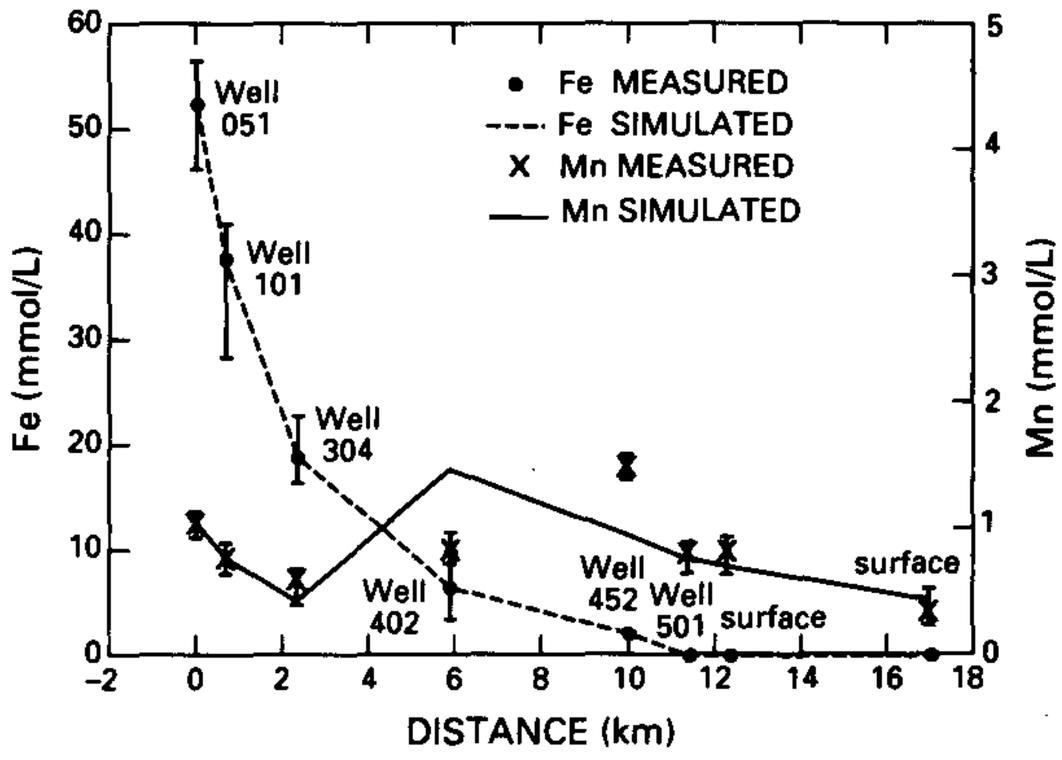

FIG. 6. Measured and simulated concentration of total dissolved Fe and Mn at observation points along flow path in aquifer. Fe(II) comprises 97% or more of total Fe.

the core of the plume at well 101, compared with the large content of Mn oxides in neutralized and uncontaminated alluvium. This observation is consistent with the depletion of MnO_2 in the column-reacted alluvium.

Two additional mechanisms affect the concentration of Fe in the aquifer. First of all, the concentration of Fe is decreased by dilution with uncontaminated groundwater. Secondly, dissolved O_2 is present in uncontaminated portions of the aquifer and can oxidize Fe(II). The only O_2 of concern in these simulations is that added to the plume by mixing with uncontaminated groundwater that contained about 0.22 mmol/l dissolved O_2. Some atmospheric O_2 also diffuses directly into the aquifer across the air–water interface; however, this process was not considered to affect the chemistry of Fe in the core of the contaminated zone. This atmospheric O_2 rapidly reacts with Mn(II) and Fe(II) near the water table and is depleted before it can reach the core of the plume.

The primary solid phase controlling the solubility of Fe in the aquifer appears to be $Fe(OH)_3$. Grains of alluvium coated with thick crusts of $Fe(OH)_3$ were identified in many cuttings from the core of the

plume. The redox state of most groundwater samples was close to the Fe^{2+}–$Fe(OH)_3$ boundary, although most Eh values were about 100–200 mV lower than equilibrium. This is not surprising considering that Fe^{3+} should be at least 10^{-5} mol/l in order to provide an exchange current at the electrode–solution interface that is great enough to establish a Nernstian Eh (STUMM and MORGAN, 1981). If the assumption that Fe(II) is in equilibrium with $Fe(OH)_3$ is accurate, the concentration of Fe^{3+} in the groundwater samples plotted in Fig. 6 would range from 10^{-7} to 10^{-9} mol/l, well below the concentration required to establish an equilibrium Eh that can be measured accurately with the platinum electrode.

The concentrations of Fe along the first 2 km of the flow path (Fig. 6) were simulated using only dilution. This is consistent with the data of FICKLIN *et al.* (1991) which indicated a lack of Mn oxides in this reach of the aquifer. From 2 to 11 km, dilution was not as significant, and oxidation by MnO_2 became the primary mechanism for removing Fe(II) from solution. The actual mass of MnO_2 in alluvium along this portion of the flow path was not known. Therefore, the quantity of MnO_2 added in each simulation was based on the amount of Fe(II) that had to be oxidized to match the measured concentration of Fe(II) in the aquifer.

Manganese

Reductive dissolution of Mn oxides by Fe(II) resulted in a net release of Mn to solution in the column experiment (Fig. 5). Manganese concentrations as high as 17.5 mmol/l were measured in the effluent, whereas the influent concentration was only 1.4 mmol/l. The total amount of Mn dissolved from the alluvium, 3.3 mmol/kg, was substantially less than the 7.1 mmol/kg predicted to dissolve by reaction (8).

Three mechanisms were considered to explain why all of the Mn(II) that should have formed by reaction 8 was not measured in effluent: (1) after partial reduction of Mn(IV) to Mn(III), a surface coating of $Fe(OH)_3$ could have formed on the Mn oxides, preventing any further reduction; (2) some Mn(II) formed by oxidation of Fe(II) may have been trapped in the porous structure of $Fe(OH)_3$. There is some evidence for such a process from the shape of the breakthrough curve in Fig. 5. After the initial spike, Mn concentrations never returned to the influent concentration. This slow leaching of Mn from the alluvium is consistent with diffusion of Mn(II) trapped in $Fe(OH)_3$ to the flowing phase: (3) Mn(II) may have precipitated with $Fe(OH)_3$ forming jacobsite [$Mn(FeO_2)_2$] or some similar mineral (CORNELL and GIOVANOLI, 1987). Sequential chemical extraction of the reacted alluvium after completion of the column experiment measured an increase of from 2.4 to 4.4 mmol/kg in the amount of Mn associated with amorphous Fe oxides. Therefore, coprecipitation of Mn with $Fe(OH)_3$ would be plausible.

Concentration histories could be simulated using the diffuse double-layer model. A log K of -2.6 (reaction 7, Table 3) gave the best fit to the experimental data. This value is relatively close to the log K of -3.5 estimated by DZOMBAK and MOREL (1990) from linear free energy relationships for adsorption of Mn on fresh amorphous $Fe(OH)_3$. The simulations correctly predicted that essentially all of the Mn in the influent as well as the Mn reduced by Fe(II) should be adsorbed at pH values greater than 7.7. As pH decreased below 7.7, adsorption decreased and the concentration of Mn in the effluent rapidly increased. Less than 1% Mn was adsorbed at pH 4.4. The Mn concentration spike between pore volumes 2 and 3 correlated with the decrease in pH and represents the Mn that was reduced by Fe(II), but was not adsorbed. In contrast to the observed effluent concentrations, the model predicted that Mn should rapidly decline to the influent concentration after depletion of the available MnO_2. No attempt was made to model the apparent diffusion-controlled leaching of Mn from alluvium between pore volumes 3 and 11.

The concentration of Mn rapidly approached the detection limit when the influent was switched back to uncontaminated groundwater. The uncontaminated groundwater contained dissolved oxygen which would be expected to reoxidize Mn(II) in the alluvium and prevent any further leaching.

Manganese behavior in groundwater and surface water was simulated by a combination of dilution, adsorption and precipitation. The decline in Mn concentration along the most acidic (pH <4) first 2 km of the flow path was successfully simulated by dilution alone (Fig. 6) and is consistent with the fact that the decrease in Fe(II) along this same stretch of aquifer could be simulated without reduction of MnO_2.

The observed increase in the concentration of Mn in groundwater between 2 and 9 km could be modeled by the reductive dissolution of MnO_2. However, initial simulations predicted <1% adsorption of Mn at wells 402 (pH = 4.18) and 452 (pH = 4.26), so the simulated Mn concentrations were much greater than those actually measured. The column data indicated that approximately 65% of the Mn reduced by Fe(II) remained in the solid phase. Therefore, the same mechanism was assumed to have occurred in the aquifer, and aqueous Mn at wells 402 and 452 was simulated by removing 65% from solution as a coprecipitate after all reactions had taken place. Subsequent modeled concentrations of Mn in solution at well 402 were still too high, and at well 452 were too low. There are not enough data on the solid phase associations of Mn or the kinetics of these reactions to accurately model Mn in this part of the aquifer.

Simulations of aqueous Mn were more accurate along the remainder of the flow path (501, Setka

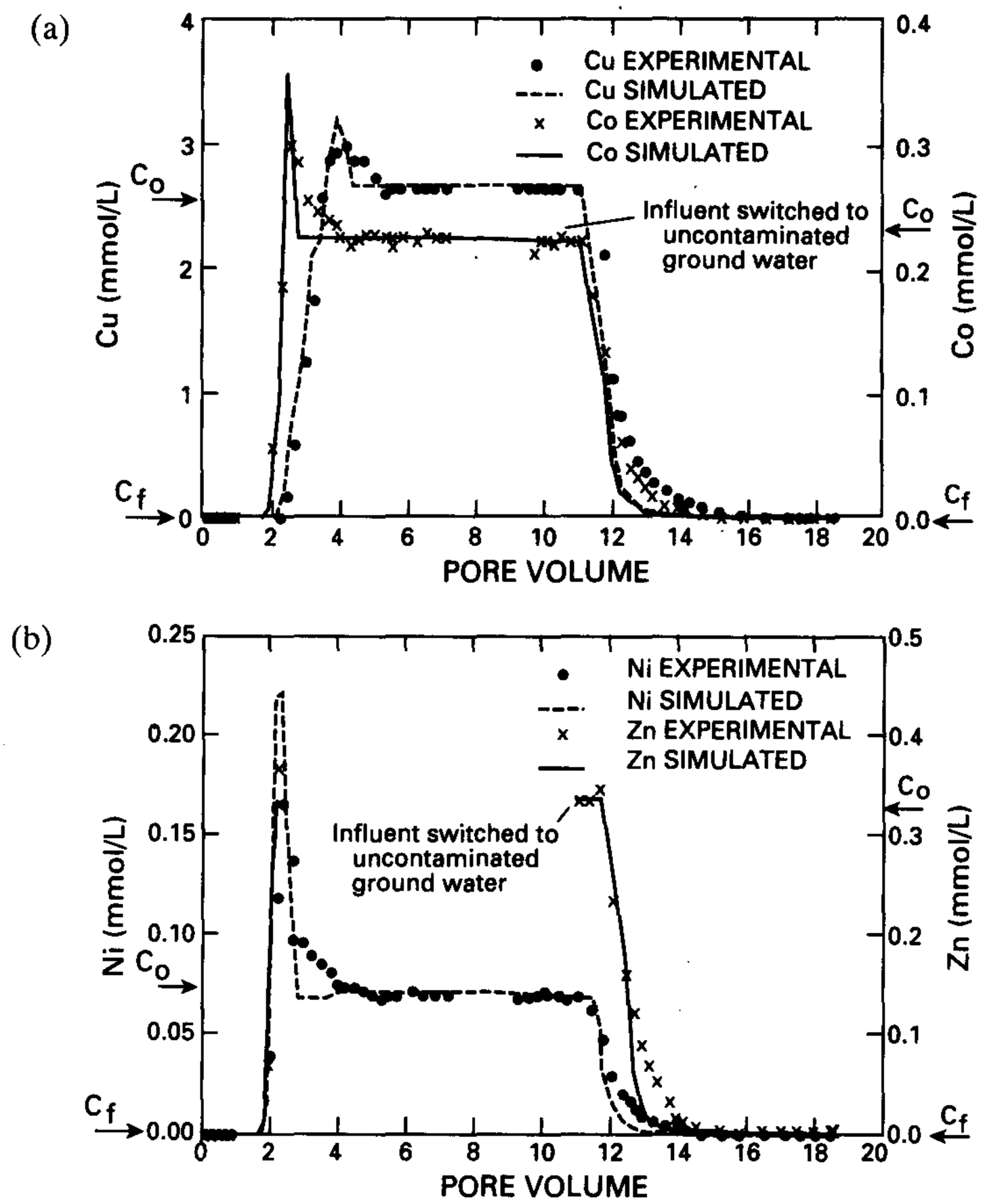

FIG. 7. (a) and (b) Experimental and simulated breakthrough curves for Cu, Co, Ni and Zn in column effluent. Zn concentrations between pore volume 2 and 11 are not shown because of the potential for Zn contamination from column apparatus at low pH.

Ranch, Inspiration Dam, Fig. 6). The decrease in Mn from 10 to 11.5 km corresponded with an increase in pH to 5.9, and was accurately simulated by adsorption using the log K determined for the column data. Groundwater discharges at the surface near 12 km and becomes oxygenated. Manganese is oxidized and precipitates as Mn oxides, coating the stream bed. The concentrations of Mn in both surface-water samples, 12 and 16 km, were simulated by assuming oxidation to birnessite.

Copper, cobalt, nickel and zinc

Experimental breakthrough curves for Cu, Co, Ni and Zn were similar and are typical of the pH-dependent adsorption of cations on oxide surfaces (Fig. 7a and b). Concentrations were below the limits of detection at pH >7, then rapidly increased as the pH of column effluent decreased. The spike in the concentration of Cu, Co and Ni can be explained by desorption as the acidic front eluted through the column. Mass balance calculations indicate that all of the Ni initially removed from solution was desorbed, compared with 25% of the Co and only 6% of the Cu. Evidence indicates that the Cu retained by the alluvium was associated with Fe oxides. The amount of Cu irreversibly adsorbed was 0.95 mmol/kg, which compares well with the 0.91 mmol/kg Cu that was chemically extracted from the reacted alluvium. Electron microprobe analyses of reacted alluvium measured as much as 10% by weight Cu associated with Fe oxides. The irreversibly adsorbed Co was also associated with Fe oxides. A concentration spike was also measured for Zn; however, preliminary leaching experiments indicated the potential for Zn contamination at low pH from some of the components used in column construction. Therefore, only the initial portion of the breakthrough curve and the rinse-out curve are plotted for Zn.

The diffuse double-layer model was used to simulate the breakthrough curves for Cu, Co, Ni and Zn. Equilibrium constants for adsorption of Cu, Ni and Zn (Table 3) are the values reported by DZOMBAK and MOREL (1990) for adsorption on $Fe(OH)_3$. The equilibrium constant for Co was adjusted to fit the experimental data. Both the pH at which the four metals were first detected in column effluent and the steep rise in concentration were accurately simulated (Fig. 7a and b). The concentration spikes were simu-

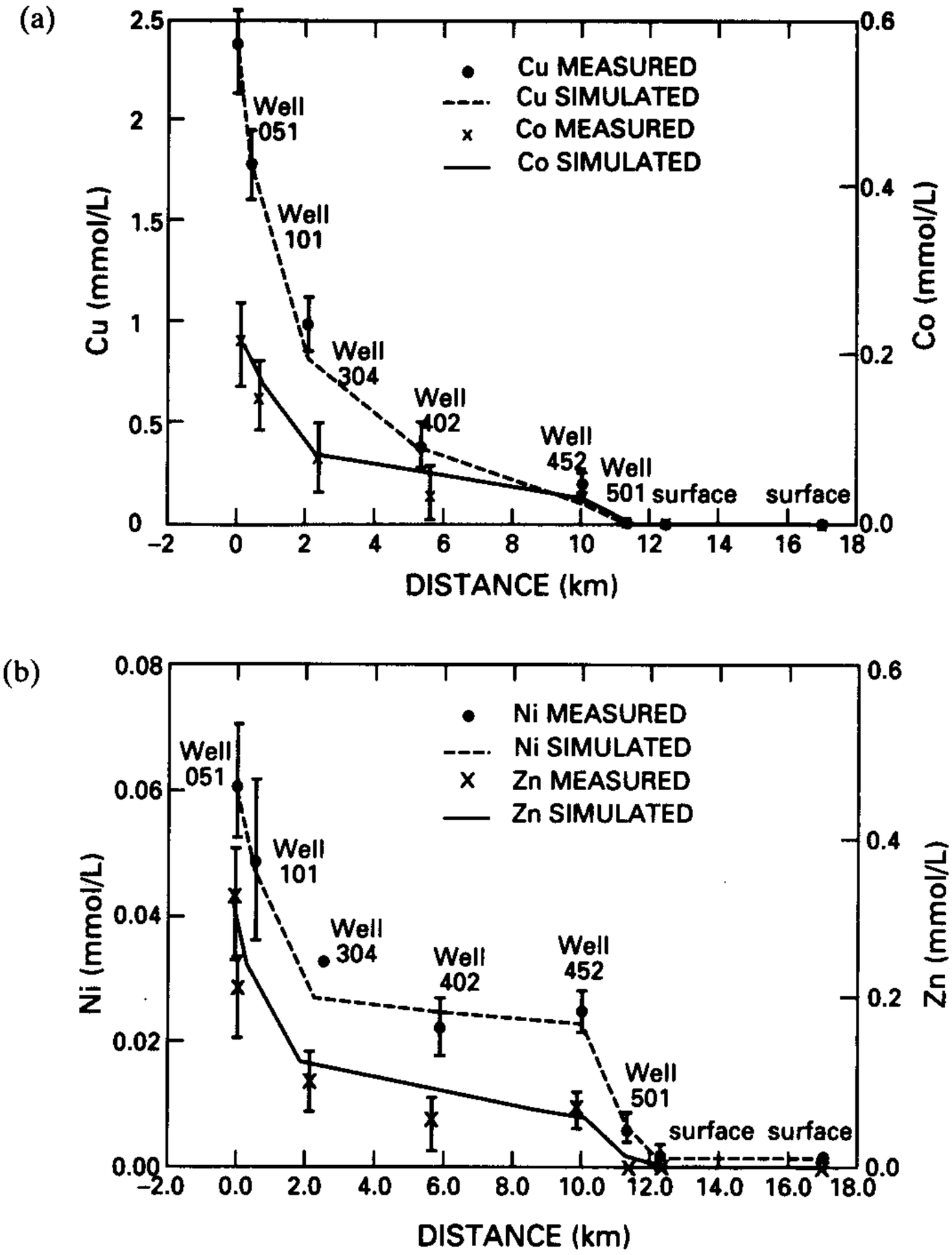

FIG. 8. (a) and (b) Measured and simulated concentrations of Cu, Co, Ni and Zn along flow path in aquifer.

lated by partially reversible adsorption. An amount of metal was allowed to desorb in the model that was equal to the amount actually measured in the column experiment. Hence, all of the Ni was allowed to desorb, but only 25% of the Co and 6% of the Cu. The model predicted essentially instantaneous desorption. Actual concentrations approached influent values more slowly and probably reflected the slower process of diffusion out of pores of stagnant water within the column. The concentrations of all four metals decreased to below detection limits within a few pore volumes after switching back to uncontaminated groundwater.

The concentrations of Cu, Co, Ni and Zn along much of the flow path in the aquifer were also a function of pH (Fig. 8a and b). The diffuse double-layer model predicted minimal adsorption of Co, Ni or Zn in the first 10 km because of the low pH. Concentrations along this part of the flow path were simulated only by dilution. The decrease in concentration down-gradient from 10 km corresponded with the increase in pH and was modeled by adsorption on $Fe(OH)_3$. Adsorption of Cu was predicted throughout the entire flow path, even in the acidic core of the plume. The combination of dilution plus adsorption accurately simulated Cu in groundwater.

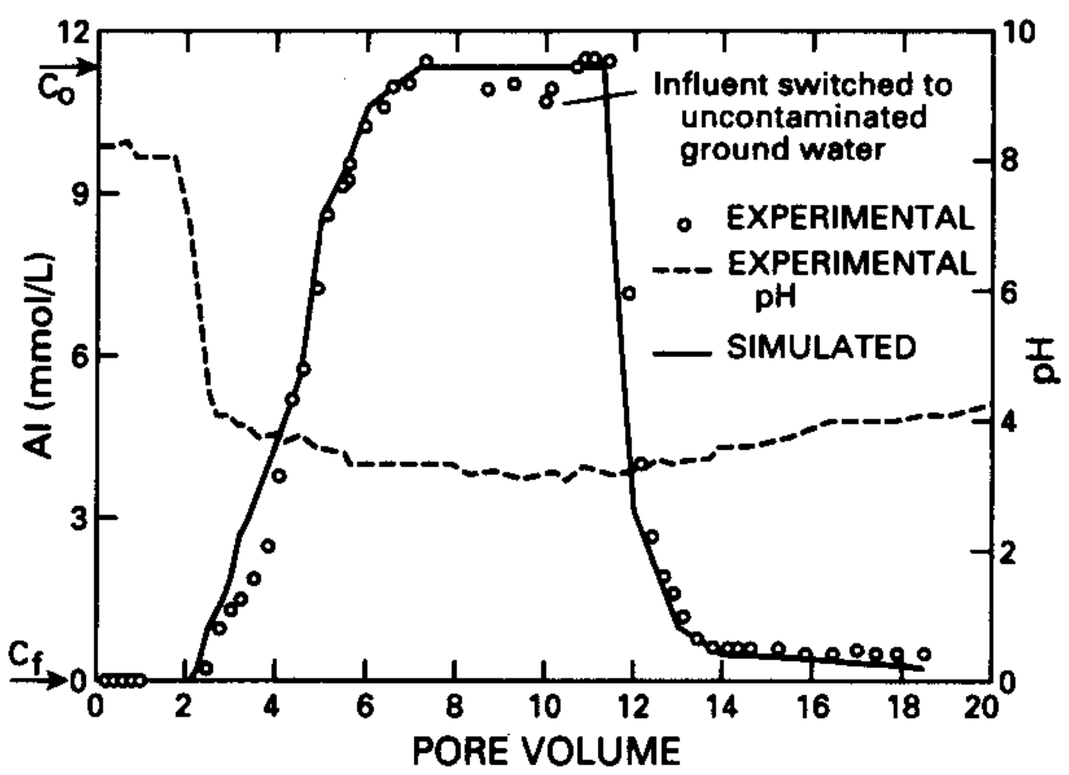

FIG. 9. Experimental and simulated concentration of Al in column effluent.

Aluminum

The concentration of Al in column effluent (Fig. 9) was a function of both pH and the concentration of SO_4. Mass balance calculations by MINTEQA2 predicted that precipitation of amorphous $Al(OH)_3$ caused the complete removal of Al from the first 2.5 pore volumes of acidic solution. As pH decreased to <4.7, several aluminum sulfate miner-

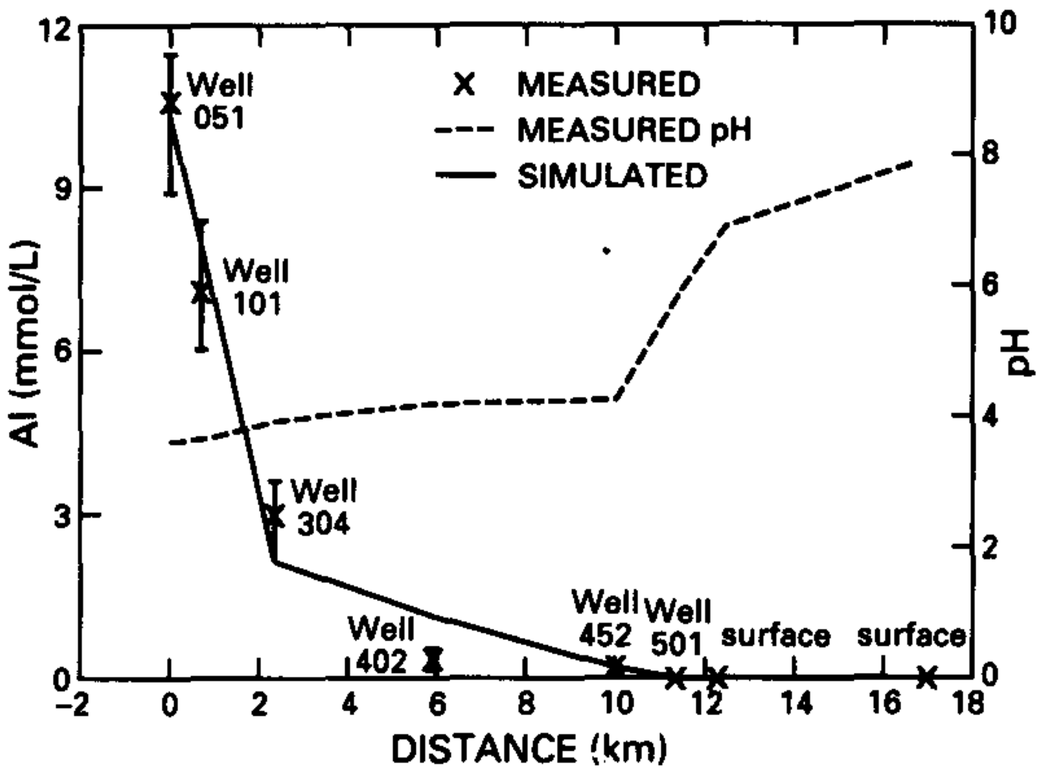

FIG. 10. Measured and simulated concentration of Al along flow path in aquifer.

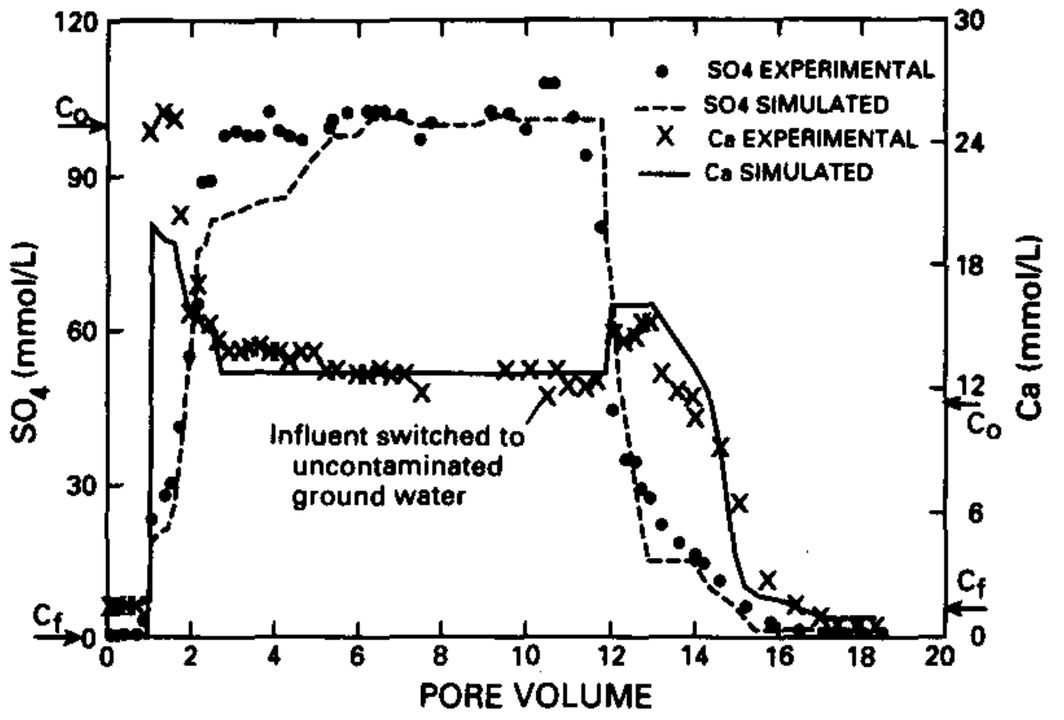

FIG. 11. Experimental and simulated concentration of Ca and SO_4 in column effluent.

als became supersaturated, including jurbanite ($AlSO_4OH \cdot 5H_2O$), alunite [$KAl_3(SO_4)_2(OH)_6$] and a basic aluminum sulfate ($AlOHSO_4$). Jurbanite has been reported to form only in environments more acidic than those in the column, and there is evidence for kinetic inhibition to precipitation of alunite at low temperatures (NORDSTROM, 1982). Therefore, neither mineral was considered to control Al solubility. Aluminum in the influent solution was in equilibrium with $AlOHSO_4$. Most effluent samples were slightly supersaturated with respect to $AlOHSO_4$, probably because of slow nucleation and precipitation.

Accordingly, $AlOHSO_4$ was used to control the solubility of Al at pH <4.7. However, the log K was changed from 3.23 to 2.2 to provide the most accurate fit to the experimental data. The use of amorphous $Al(OH)_3$ at pH >4.7, and $AlOHSO_4$ at pH <4.7 yielded an excellent match of the experimental breakthrough curve. MINTEQA2 simulations also indicated that the $Al(OH)_3$ which precipitated initially, should have dissolved and reprecipitated as $AlOHSO_4$ as the low pH, SO_4-rich water eluted through the column.

Aluminum in the interstitial pore water was rapidly rinsed from the column initially; however, concentrations levelled off at about 0.6 mmol/l by pore volume 14. The experimental data from pore volume 12 through to 18 were modeled by allowing dissolution of $AlOHSO_4$. By pore volume 18, only 10% of the $AlOHSO_4$ in the column had dissolved. Thus, a significant reservoir of Al remained in the alluvium and was predicted to continually leach into solution so long as pH remained low. As pH increased, amorphous $Al(OH)_3$ regained control over Al solubility.

The combination of amorphous $Al(OH)_3$ and $AlOHSO_4$ as controls on aqueous Al concentration worked reasonably well in simulating Al concentrations along the flow path in the aquifer (Fig. 10). The simulated concentrations plot within the range of Al concentrations measured in the aquifer with the exception of well 402 at 5.8 km. $AlOHSO_4$ controlled solubility along the first 10 km where pH was <5. Precipitation of gibbsite maintained Al below detection limits along the remainder of the flow path.

Calcium and sulfate

The concentration of Ca and SO_4 in the acidic groundwater used in the column experiment were close to equilibrium with gypsum ($CaSO_4 \cdot 2H_2O$), and concentrations in the column effluent were simulated reasonably well by maintaining equilibrium with gypsum (Fig. 11). As acidic water moved through the column, dissolution of calcite initially released a large amount of Ca. Although much of this Ca precipitated with SO_4, concentrations as high as 26 mmol/l were measured in the effluent. This is more than twice the concentration in the influent solution. Sulfate concentrations were kept low initially as gypsum precipitated. As carbonates were depleted, Ca decreased and SO_4 increased until influent concentrations were attained.

Effluent from the column was apparently supersaturated with respect to gypsum and gypsum precipitated in the collection tubes. As a result, calculations assuming equilibrium with gypsum predicted that there should have been less Ca and SO_4 in solution than was actually measured between pore volumes 1 and 5. The kinetics of gypsum precipitation in this system appeared to be a function of ionic strength. As ionic strength increased, the degree of supersaturation decreased and the simulated concentrations approached the experimental values.

Gypsum began to dissolve when uncontaminated groundwater was eluted through the column. All of the gypsum initially precipitated was dissolved by pore volume 17, and Ca and SO_4 concentrations decreased to the influent values of uncontaminated water.

There is evidence that gypsum precipitates in the aquifer. Most gypsum identified in cuttings from the aquifer was cryptocrystalline; however, selenite blades up to 1 cm long have been identified in some parts of the acidic plume. Growth of such large

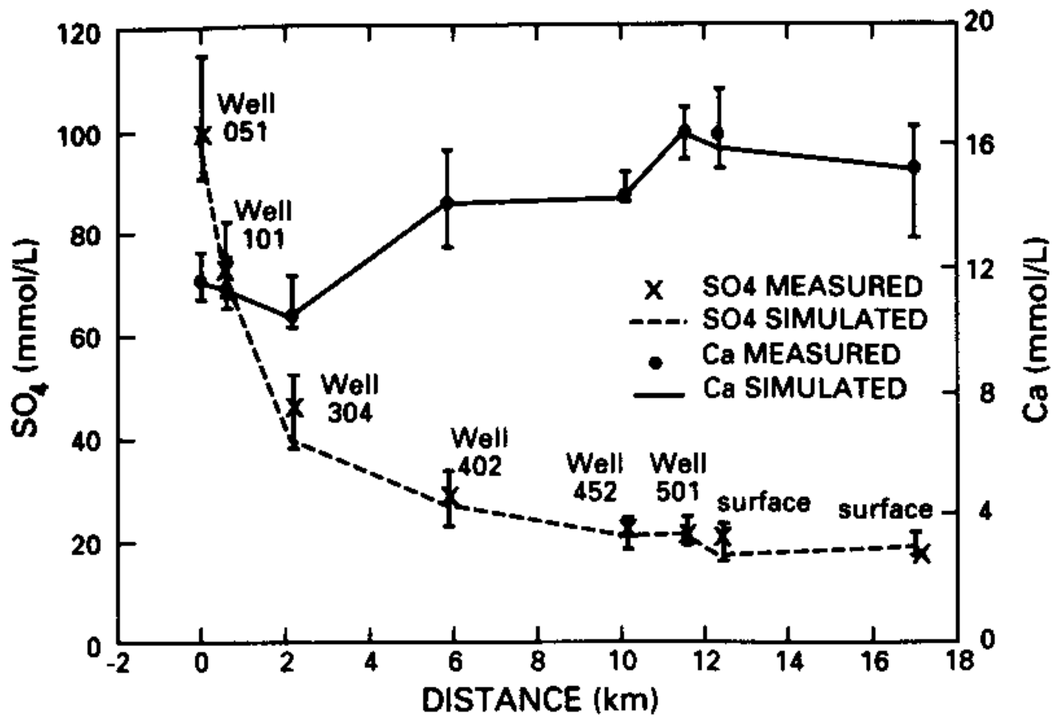

FIG. 12. Measured and simulated concentration of Ca and SO_4 along flow path in aquifer.

crystals was probably related to zones rich in carbonate minerals whose dissolution provided a continuous source of Ca.

Simulations by MINTEQA2 predicted gypsum precipitation at each point along the flow path except for the last one at 17 km where gypsum was undersaturated (Fig. 12). The concentration of Ca increased along the flow path reflecting dissolution of calcite and dolomite. Precipitation of gypsum and $AlOHSO_4$ and dilution caused SO_4 concentrations to decrease.

CONCLUSIONS

A geochemical model was developed to describe the evolution of a plume of acidic groundwater in an alluvial aquifer. Reactions that controlled the concentration of selected constituents were identified by evaluating groundwater analyses in conjunction with data from laboratory experiments. The model was calibrated first by adjusting reaction hypotheses and equilibrium constants in order to match concentrations in breakthrough curves from a laboratory column experiment. Then, the model was used to simulate the change in groundwater composition along a one-dimensional flow path in the aquifer. In some cases, lack of thermodynamic equilibrium made modeling difficult. The main conclusions are as follows.

(1) Chloride was shown in experiments to be nonreactive and therefore could be used to estimate the amount of dispersion in breakthrough curves from the column experiment and the amount of dilution of the acidic plume in the aquifer.

(2) H^+ was neutralized primarily by reaction with carbonate minerals. These reactions were relatively rapid and resulted in a steep pH gradient over a short distance. In parts of the aquifer where carbonates were depleted and pH was <4.5, adsorption of ferrihydrite was the dominant control on pH and formed an important reservoir of H^+. Reaction with silicate minerals may have some effect on pH; however, reaction rates are probably too slow to have any significant effect on pH.

(3) The concentration of Fe in groundwater was controlled by oxidation of Fe(II) to Fe(III) and precipitation of $Fe(OH)_3$. In the column experiment, Mn(III,IV) oxides were the only apparent oxidants. In the aquifer, Fe(II) was oxidized by a combination of Mn oxides and dissolved oxygen in uncontaminated groundwater that mixed with the plume.

(4) Reduction of Mn by Fe(II) increased the concentration of Mn in column effluent and groundwater. Some of this Mn was adsorbed by $Fe(OH)_3$ at higher pH values. Desorption occurred as pH decreased. A significant fraction of the Mn remained associated with the solid phase, either as a coprecipitate or an incompletely reduced oxide.

(5) The concentration of aqueous Cu, Co, Ni and Zn were a function of pH. Adsorption of these metals was simulated using the diffuse layer surface-complexation model.

(6) Aluminum was controlled by precipitation of $Al(OH)_3$ at pH >4.7. $AlOHSO_4$ appeared to control solubility at lower pH values.

(7) Calcium and sulfate concentrations were controlled by precipitation of gypsum.

The column experiment also provided useful information about the potential fate of contaminants in the aquifer after the source of acidic water is eliminated. Values of pH are likely to remain low for a substantial time because of dissociation of the $\equiv FeOH\text{–}H^+$ complex. Aluminum may also pose a long-term threat to water quality because of $AlOHSO_4$ dissolution. While pH values remain below 4.6, precipitation of $Al(OH)_3$ is unlikely, resulting in increased Al concentrations. Dissolution of gypsum will result in higher concentrations of Ca and SO_4; however, most of the gypsum should be removed within a few pore volumes. Any Fe, Mn, Cu, Co, Ni or Zn associated with alluvium in the acidic portion of the plume should remain relatively immobile, and the concentration of these constituents should rapidly return to background levels.

The reactions used in this model represent one plausible set of reactions that were able to successfully simulate breakthrough curves from the column experiment as well as the change in the composition of groundwater in the aquifer. Some of the reactions could be demonstrated from analysis of the field data, whereas other reactions only became evident through analyzing data from carefully controlled laboratory experiments.

Acknowledgements—Thanks are extended to James Eychaner for the overall coordination of this study and help with sample collection, John Garbarino for assistance with cation analyses, and Robert Heinzman for determination of alluvial mineralogy. The manuscript was improved greatly by the reviews by Doug Kent, James Brown, John Hem and James Tindall.

Editorial handling: Yousif Kharaka.

REFERENCES

ALLISON J. D., BROWN D. S. and NOVO-GRADAC K. J. (1991) MINTEQA2/PRODEFA2, A geochemical assessment model for environmental systems: Version 3.0 user's manual. U.S. Environmental Protection Agency Report No. EPA/600/3-91/021.

ASGHAR M. and KANEHIRO Y. (1981) The fate of applied iron and manganese in an oxisol and an ultisol from Hawaii. *Soil Sci.* **131**, 53–55.

BAHR J. M. and RUBIN J. (1987) Direct comparison of kinetic and local equilibrium formulations for solute transport affected by surface reactions. *Water Resour. Res.* **23**, 438–452.

BROWN J. G. (1990) Chemical, geologic, and hydrologic data from the study of acidic contamination in the Miami Wash–Pinal Creek Area, Arizona, water years 1988–89. *U.S. Geol. Surv. Open-File Rep.* 90-395.

CHAO T. T. (1972) Selective dissolution of manganese oxides from soils and sediments with acidified hydroxylamine hydrochloride. *Proc. Soil Sci. Am.* **36**, 764–768.

CHAO T. T. and ZHOU L. (1983) Extraction techniques for selective dissolution of amorphous iron oxides from soils and sediments. *Soil Sci. Soc. Am. J.* **47**, 225–232.

CORNELL R. M. and GIOVANOLI R. (1987) Effect of manganese on the transformation of ferrihydrite into geothite and jacobsite in alkaline media. *Clays Clay Minerals* **35**, 11–20.

DREIMANIS A. (1962) Quantitative gasometric determination of calcite and dolomite by using Chittick apparatus. *J. Sedim. Petrol.* **32**, 520–529.

DZOMBAK D. A. and MOREL F. M. M. (1990) *Surface Complexation Modeling*. John Wiley & Sons, New York.

ENVIROLOGIC SYSTEMS, INC. (1983) Mining activities and water-quality report. Central Arizona Association of Governments Mineral Extraction Task Force Report METF-7, Florence, Arizona.

EYCHANER J. H. (1988) Evolution of acidic groundwater contamination in a copper-mining area in Arizona. In *Proc. Computer Methods and Water Resources, First International Conference, Morocco*, Vol. 6, pp. 291–302. Springer, New York.

EYCHANER J. H. (1989) Movement of inorganic contaminants in acidic water near Globe, Arizona. U.S. Geol. Surv. Water Resour. Invest. Rep. 88-4220, pp. 567–575.

EYCHANER J. H. (1991) The Globe, Arizona Research Site—contaminants related to copper mining in a hydrologically integrated environment. *U.S. Geol. Surv. Water Resour. Invest. Rep.* 91-4043, pp. 439–447.

EYCHANER J. H., REHMANN M. R. and BROWN J. G. (1989) Chemical, geologic, and hydrologic data from the study of acidic contamination in the Miami Wash–Pinal Creek area, Arizona, water years 1984–1987. *U.S. Geol. Surv. Open-File Rep.* 89-410.

EYCHANER J. H. and STOLLENWERK K. G. (1985) Neutralization of acidic groundwater near Globe, Arizona. In *Proc. Groundwater Contamination and Reclamation Symposium, Tucson, Arizona*, pp. 141–148. Am. Water Resourc. Ass.

FICKLIN W. H., LOVE A. H. and PAPP C. S. E. (1991) Solid phase variations in an aquifer as the aqueous solution changes, Globe, Arizona. *U.S. Geol. Surv. Water Resourc. Invest. Rep.* 91-4034, pp. 475–480.

GOLDEN D. C., DIXON J. B. and CHEN C. C. (1986) Ion exchange, thermal transformations, and oxidizing properties of birnessite. *Clays Clay Minerals* **34**, 511–520.

HEM J. D. and LIND C. J. (1983) Nonequilibrium models for predicting forms of precipitated manganese oxides. *Geochim. cosomochim. Acta* **47**, 2037–2046.

KRISHNAMURTI G. S. R. and HUANG P. M. (1987) The catalytic role of birnessite in the transformation of iron. *Can. J. Soil Sci.* **67**, 533–543.

NAUMOV G. B., RYZHENKO B. N. and KHODAKOVSKY I. L. (1974) Handbook of Thermodynamic Data. U.S. Department of Commerce, NTIS Report PB-226 722.

NORDSTROM D. K. (1982) The effect of sulfate on aluminum concentrations in natural waters: some stability relations in the system Al_2O_3–SO_3–H_2O at 298 K. *Geochim. cosmochim. Acta* **46**, 681–692.

NORDSTROM D. K., JENNE E. A. and BALL J. W. (1979) Redox equilibria of iron in acid mine waters. In *Chemical Modeling in Aqueous Systems* (ed. E. A. JENNE). *Am. chem. Soc. Symp. Ser.* **93**, 51–79.

NORDSTROM D. K., PLUMMER L. N., LANGMUIR D., BUSENBERG E., MAY H. M., JONES B. F. and PARKHURST D. L. (1990) Revised chemical equilibrium data for major water–mineral reactions and their limitations. In *Chemical Modeling of Aqueous Systems II* (eds D. C. MELCHIOR and R. L. BASSETT). *Am. chem. Soc. Symp. Ser.* **416**, 398–413.

PARKHURST D. L., THORSTENSON D. C. and PLUMMER L. N. (1980) PHREEQE—A computer program for geochemical calculations. *U.S. Geol. Surv. Water Resourc. Invest. Rep.* 80–96.

PETERSON N. P. (1962) Geology and ore deposits of the Globe–Miami District, Arizona. *U.S. Geol. Survey Prof. Paper* 342.

POSTMA D. (1985) Concentration of Mn and separation from Fe in sediments — I. Kinetics and stoichiometry of the reaction between birnessite and dissolved Fe(II) at 10°C. *Geochim. cosmochim. Acta* **49**, 1023–1033.

SELLERS W. D., HILL R. D. and SANDERSON-RAE M. (1985) Arizona climate, the first hundred years. University of Arizona, Tucson.

STUMM W. and MORGAN J. J. (1981) *Aquatic Chemistry* (2nd ed.). John Wiley and Sons, New York.

US EPA (1987) Finding of violation and order. Docket No. IX-FY86-78. U.S. Environmental Protection Agency.

USGS (1979) Techniques of Water-resources Invest. U.S. Geol. Surv. Methods for Determination of Inorganic Substances in Water and Fluvial Sediments. Book 5, Chap. A1. U.S. Geol. Surv. Washington, DC.

USGS (1989) Techniques of Water-resources Invest. U.S. Geol. Surv. Methods for Determination of Inorganic Substances in Water and Fluvial Sediments. Book 5, Chap. A1. U.S. Geol. Surv. Washington, DC.

WALTER G. R. and NORRIS J. R. (1991) Hydrochemical zoning in the Pinal Creek alluvium. *U.S. Geol. Surv. Water Resourc. Invest. Rep.* 91-4043, pp. 516–519.